ELSEVIER

Journal of Chromatography B, 698 (1997) 133–145

JOURNAL OF CHROMATOGRAPHY B

Buspirone metabolite structure profile using a standard liquid chromatographic–mass spectrometric protocol

Edward H. Kerns[a,*], Robyn A. Rourick[b], Kevin J. Volk[b], Mike S. Lee[c]

[a]*Bristol-Myers Squibb Pharmaceutical Research Institute, Building 105, 1 Squibb Drive, P.O. Box 191, New Brunswick, NJ 08903-0191, USA*

[b]*Bristol-Myers Squibb Pharmaceutical Research Institute, Wallingford, CT 06492, USA*

[c]*Bristol-Myers Squibb Pharmaceutical Research Institute, Princeton, NJ 08540, USA*

Received 24 September 1996; received in revised form 14 April 1997; accepted 15 April 1997

Abstract

A rapid and systematic LC–MS protocol is utilized to profile buspirone metabolites. Analysis of rat bile, urine and liver S9 samples using a standard LC–MS method provides structural information for 25 metabolites. The resulting buspirone metabolite structure database contains characteristic retention time, molecular mass and MS–MS product ion information for each compound. Metabolites are categorized according to profile groups, which illustrate that substitution reactions are primarily associated with the azaspirone decane dione and pyrimidine substructures. Structures of new buspirone metabolites are reported and include the despyrimidinyl, despyrimidinylpiperazine, glucuronide, hydroxyglucuronide (four isomers), methoxyglucuronide and hydroxymethoxyglucuronide (two isomers) buspirone metabolites. © 1997 Elsevier Science B.V.

Keywords: Buspirone

1. Introduction

An important milestone in the development of a new drug is the metabolite structure profile. Early assessment is critical, since the duration of action is dependent on structural modifications induced by in vivo metabolizing systems. Early knowledge of the metabolic products allows for metabolism guided structure modification schemes, whereby synthetic blockade or modification of metabolically active sites have achieved prolonged drug action. (This is complementary to lipophilicity or degradation guided structure modification to reduce clearance or increase drug stability, respectively.) Metabolites may also possess pharmacological or toxicological activity. Thus, the metabolite structure profile provides an essential perspective for the synthetic refinement and selection of drug candidates from among an extensive series of potential structures, resulting in optimum drug effectiveness and safety.

Current pharmaceutical research strategies involving combinatorial chemistry, high throughput screening and gene sequencing have greatly increased the pace of drug candidate compound generation and significantly reduced the discovery period for lead candidate selection. Organizational strategies have also decreased the time preceding Investigational New Drug (IND) filing. Preclinical research, involving the evaluation of thousands of analogs, focuses on various selection criteria which deal with activity,

*Corresponding author.

0378-4347/97/$17.00
PII S0378-4347(97)00254-5

metabolism, bioavailability, stability and process feasibility. Traditional strategies for metabolite profiling have focused on methods utilizing radiolabeled tracer technology, sample scale-up, extraction, HPLC fraction collection and spectroscopic analysis of each component. This approach has yielded an effective body of information for regulatory and basic research purposes, however, these methods present analytical limitations in terms of speed and efficiency necessary for current pre-clinical research. Thus, metabolite profiling strategies should incorporate rapid, high-throughput analytical methods for early assembly of metabolite structure profiles supporting the short time frame and tremendous volume of candidate samples generated under accelerated drug discovery paradigms. By rapidly obtaining metabolic structural information, the more time-consuming studies (e.g., quantitative pharmacokinetics assays [21–25], formulation, stability, process scale-up) may be reserved for more detailed study of the most promising drug candidates.

Mass spectrometric (MS) techniques offer comparative advantages for speed and productivity for pharmaceutical analysis. A survey of components in a complex pharmaceutical research sample and their molecular masses (M_r) can be provided using combined liquid chromatography–mass spectrometry (LC–MS) without pre-fractionation. Further structural detail can be provided using liquid chromatography–tandem mass spectrometry (LC–MS–MS). This approach has been successfully applied in various fields of pharmaceutical research, such as natural products [1–3], impurities and degradants [4,5] and metabolites [6–13]. Structure elucidation of drug metabolites using MS–MS [14–17] is based on the premise that metabolites retain substructures of the parent drug molecule and, thus, produce MS–MS product ions associated with those substructures. Using the parent drug as a substructural template, metabolite structures present in crude mixtures may be rapidly characterized and often identified without standards for each metabolite. Utilization of the ionspray LC–MS interface [18] allows for the consistent analysis of labile and polar phase II metabolites at trace levels compared to earlier LC–MS interfaces (e.g., thermospray) due to the low internal energy imparted to the analyte and eliminates the necessity of deconjugation prior to analysis [9].

We have applied LC–MS techniques to obtain a profile of the metabolites of buspirone for on-going phase IV research. Buspirone (Fig. 1) is widely used in anxiolytic therapy [19,20]. Detailed studies on the electron ionization (EI) MS of buspirone [21], quantitative MS methods and detailed studies on the metabolites of buspirone [22–25] have been previously reported.

This buspirone metabolite study has been completed using LC–MS techniques in combination with a strategy for rapid, high-throughput LC–MS analysis, which is consistent with current pharmaceutical research trends. This strategy incorporates minimal sample preparation for reduced time and sample size, as well as reduced degradation of labile components. A rapid standard HPLC method has been locked-in for this and related studies on this drug, allowing for automation, rapid sequencing between samples (without consuming time to change conditions) and reproducibility throughout the lifetime of the drug. Finally, a metabolite structure database has been assembled to speed characterization of other buspirone-derived structures. Each of the analytical steps (preparation, LC–MS and LC–MS–MS) is completed in 30 min or less, thus, integrating traditional bench-scale mixture analysis steps (i.e., scale-up, extraction, fractionation and individual component spectroscopic analysis) into a single micro-scale instrumental technique for rapid analysis.

Using this strategy, a buspirone metabolite profile encompassing 25 structures has been obtained. Several previously unknown phase I and phase II metabolites were observed. The resulting buspirone metabolite structure database contains information on the structure, M_r, UV characteristics, relative retention time (t_{RR}) and MS–MS product ion spectrum of these metabolites, which will be useful for future studies involving buspirone, such as clinical therapy.

2. Experimental

2.1. Materials

2.1.1. Chemicals

Solvents and buffer reagents were HPLC grade from Fisher (Fairlawn, NJ, USA). S9 incubation

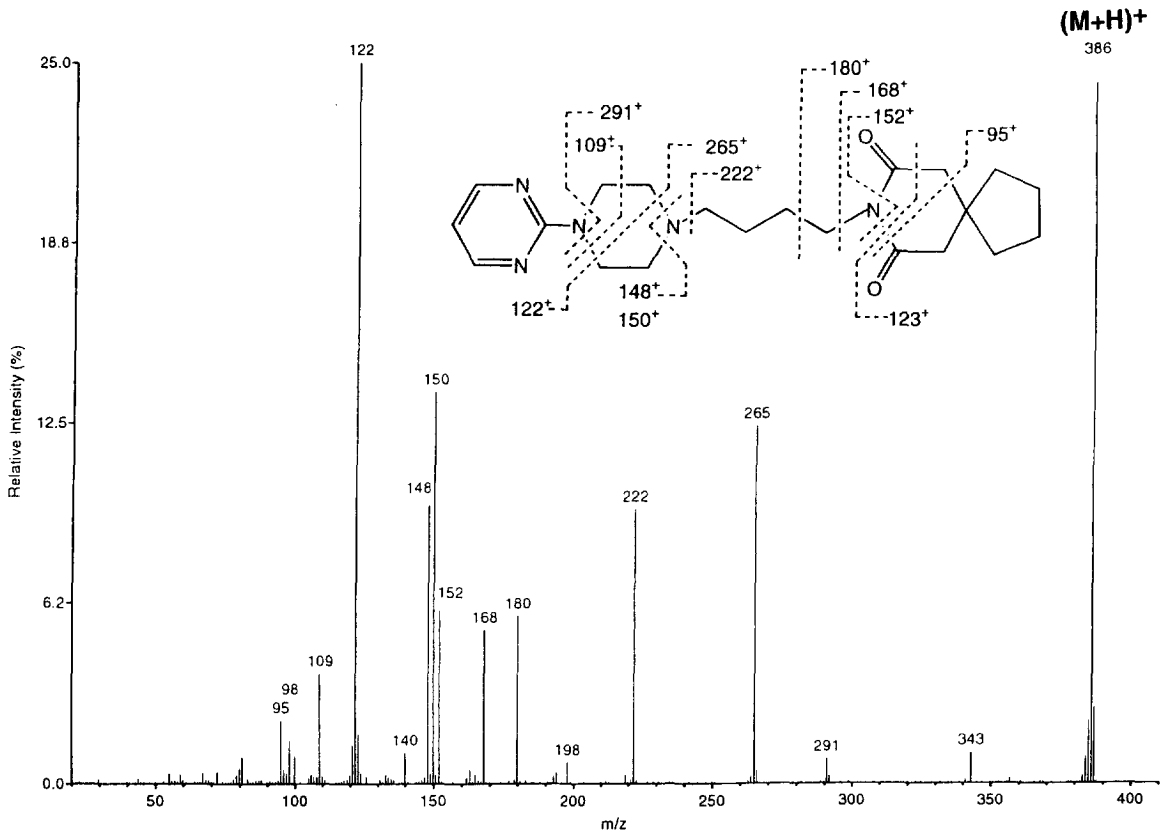

Fig. 1. Structure and ionspray MS–MS product ion spectrum of buspirone protonated molecule $(M+H)^+$ at m/z 386. The MS–MS fragmentation of buspirone was used as the 'template' for proposal of buspirone metabolite structures. The product ions associated with specific substructures are shown.

reagents were from Sigma (St. Louis, MO, USA). Buspirone HCl was synthesized in-house.

2.1.2. Samples

Two male Sprague–Dawley rats from Hilltop Laboratory Animals (Scottsdale, PA, USA) weighing approximately 300 g were anaesthetized and their bile ducts were cannulated using a length of PE10 tubing. They were each given a dose of 10 mg of buspirone HCl in 1 ml of water via gavage after a 1-h recovery. The rats were housed in metabolism cages. Urine and bile was collected over the 0–4 h course of the study and pooled. Samples were stored at −20°C until prepared for instrumental analysis.

Male Sprague–Dawley rat S9 preparation was obtained from In Vitro Technologies (Baltimore, MD, USA). The protein content was approximately 20 mg/ml. Aliquots (250 μl) of S9 preparation were incubated in a total volume of 1 ml of 1.0 *M* potassium phosphate buffer (pH 7.4) containing 25 μg of buspirone, 0.85 mg of $NADP^+$, 1.5 mg glucose-6-phosphate, 2 units of glucose-6-phosphate dehydrogenase, 25 μl of nicotinamide solution in 0.6 *M* phosphate buffer and 50 μl of magnesium chloride solution in 0.1 *M* phosphate buffer. The incubations were conducted in a heating block at 37°C for 2 h following the addition of buspirone.

2.2. Sample preparation

Samples were diluted 1:1 with acetonitrile in an Eppendorf vial. The vial was then centrifuged at 6000 *g* for 5 min. An 8-μl aliquot of liquid sample

supernatant was injected into the HPLC column for LC–MS or LC–MS–MS analysis.

2.3. Liquid chromatography

Standard HPLC chromatographic conditions which we have found useful for LC–MS analysis of a wide variety of samples from pharmaceutical research and development were utilized. A MacMod (Chadds Ford, PA, USA) Zorbax RX C_{18} reversed phase column (150 mm×2.1 mm×3 μm) was used. The mobile phase program consisted of a linear gradient from 90:10 buffer (2 m*M* ammonium acetate, pH 5.0)–acetonitrile (ACN) to 10:90 buffer–ACN over 15 min at a flow-rate of 0.3 ml/min, followed by a 2.0 min hold at 10:90 buffer–ACN. UV spectra and UV chromatograms (260 nm) were obtained using the diode array detector on-line between the HPLC column and the mass spectrometer.

2.4. Mass spectrometry

Analyses were performed using a PE Sciex (Concord, Ontario, Canada) API III tandem quadrupole mass spectrometer equipped with an ionspray LC–MS interface. A Hewlett–Packard (Avondale, PA, USA) HP1090M system equipped with a UV diode array detector was used for HPLC. Analyses were automated by integration of the HPLC with the MS control computer. The HPLC column eluent flowed directly into a diode array UV detector, and then into the mass spectrometer using a 4:1 split. The ionspray tip was operated at +5200 v. Full scan mass spectra were obtained while continuously scanning from *m/z* 150 to *m/z* 1200 with a step size of 0.4 u and a dwell time of 1.0 ms. MS–MS product ion spectra were produced by collision induced dissociation (CID) of the protonated molecule $(M+H)^+$ ion of each analyte at their respective HPLC retention times. CID utilized argon collision gas at $450 \cdot 10^{12}$ atoms/cm^2 and a collision energy of 50 eV. MS–MS product ion spectra were obtained while scanning Q3 from *m/z* 50 to approximately *m/z* 20 greater than the protonated molecule $(M+H)^+$. Mass spectral information was readily obtained for approximately 50 ng and greater of each component in the mixture injected into the LC–MS system.

2.5. Procedure

The procedure utilized for metabolite profiling can be summarized as follows:

(1) Analyze the drug standard (approximately 200 ng) using full scan LC–MS using the standard conditions. The production of an abundant $(M+H)^+$ ion, characteristic of the drug's M_r, and retention time are verified. The relative retention time (t_{RR}) for the drug is defined as 1.00.

(2) Obtain the MS–MS product ion spectrum of the drug standard at its HPLC retention time. Associate the MS–MS product ions with specific drug molecule substructures as a 'template' for interpreting the structures of metabolites.

(3) Analyze each acetonitrile-treated crude mixture sample using full scan LC–MS to obtain the t_{RR} and M_r of each component. Individual components are noted from the total ion current chromatograms, UV chromatograms and the mass chromatograms of predictable metabolic products (e.g., +16 u for hydroxylation, +96 u for sulphation, −36 u for acetylated despyrimidinyl compound). Note the separation of isobaric metabolites.

(4) Compare the M_r and t_{RR} of each component to the database of previously elucidated metabolites for rapid dereplication of known structures.

(5) Obtain the MS–MS product ion spectrum of each unknown component at its respective retention time using LC–MS–MS.

(6) Derive structures for the metabolites by comparing their MS–MS product ion spectra to the drug 'template'. Metabolite structures are proposed based on the premise that metabolites retain substructures of the parent compound and undergo similar MS–MS fragmentations to produce product ions and neutral losses associated with those substructures [14–17]. Differences in the ions indicate modification of a specific substructure(s). The sequential loss of ions and neutral losses provide evidence of 'molecular connectivity' of substructures.

(7) Add new metabolite structures and their respective data to the structure database for use in the rapid dereplication of structures in future samples and to aid the rapid interpretation of unknown structures.

(8) Categorize metabolite structures into 'profile

groups' [3] to characterize major routes and substructures associated with the metabolic reactions.

3. Results and discussion

A metabolite structure profile of 25 buspirone metabolites from rat bile, urine and liver S9 has been obtained. A summary of buspirone metabolites observed in these studies is presented in Table 1. These structures result from diverse metabolic reactions including hydroxylation, N-dealkylation, catechol O-methylation and glucuronidation. In many cases the structures indicate the occurrence of multiple metabolic reactions. These results are consistent with the metabolite structures previously reported for buspirone [22–25]. In addition, many new buspirone metabolite structures are observed. These include the N-dealkylation products despyrimidinyl buspirone and despyrimidinyl piperazine buspirone, as well as glucuronide conjugates. The MS–MS product ion spectra of the metabolites are summarized in Table 2. In combination with Table 1, these results provide a buspirone metabolite structure database indexed by analytical characteristics.

The LC–MS protocol integrates HPLC separation, UV diode array detection, ionspray MS and MS–MS in one instrumental configuration to rapidly profile metabolite structures. The HPLC analysis of the complex physiological sample provides a primary stage of metabolite separation. A molecular mass profile of the sample components which may be metabolites is assembled by examining the full scan mass spectra of the peaks in the LC–UV, LC–MS total ion chromatogram and the LC–MS selected ion chromatograms (for predictable metabolic products) as in step 3 above. (LC–UV chromatograms of samples and controls have not been shown here for brevity). HPLC resolution of components, however, is not necessary for independent structural analysis using ionspray MS and MS–MS. Structure elucidation relies, first, on observing the M_r of each component. Unresolved components exhibiting different M_r values are 'mass resolved' by MS even if they are not time resolved by HPLC. HPLC separation is useful in separating isobaric metabolites for independent analysis. For example, the mass chromatograms of selected metabolites in the rat bile sample are shown in Fig. 2. Four isobaric hydroxy buspirone metabolites having an $(M+H)^+$ at m/z 402 are separated using HPLC. Separate MS–MS product ion spectra of the individual hydroxy metabolites have been obtained.

Full scan mass spectra of buspirone metabolites produced by ion-spray have abundant $(M+H)^+$ ion signal with little detectable fragmentation. Therefore, the observed ions provide reliable M_r confirmation. Even the labile phase II conjugated buspirone metabolites produce strong $(M+H)^+$ ion signal without the production of deconjugated ions commonly observed using other MS ionization methods, such as fast atom bombardment and thermospray which produce significant aglycone ion signal. For example, the full scan spectrum of hydroxy buspirone glucuronide in Fig. 3 contains a strong $(M+H)^+$ ion at m/z 594 with no observed deconjugated ion at m/z 418.

The MS–MS product ion spectrum of buspirone is shown in Fig. 1. The ions and neutral losses associated with diagnostic substructures of buspirone are indicated. The product ion at m/z 122, for example, is indicative of the pyrimidine substructure. The presence of this ion in the MS–MS product ion spectrum of a metabolite indicates a structure containing a pyrimidine substructure. Similarly, the m/z 180 product ion is diagnostic of the azaspirone decane dione substructure and the neutral loss of 164 (producing the m/z 222 ion in buspirone) is diagnostic of the butyl azaspirone decane dione substructure.

The MS–MS substructural elucidation scheme provides for the rapid categorization of metabolites into 'profile groups' [3]. Using this approach metabolite structures can be grouped to reflect structural substitutions resulting from specific metabolic reactions. Profile groups directly correlate specific MS–MS product ions and neutral losses with the presence, absence, substitution and molecular connectivity of specific buspirone substructures and their modification. Profile groups have been identified with abbreviations corresponding to specific substructures: azaspirone decane dione (A), butyl piperazine (B) and pyrimidine (P). A substituted substructure is designated with the subscript s and a hyphen denotes substructure connectivity. Thus, A_s-B-P refers to metabolites which contain the A, B and

Table 1
Buspirone metabolites identified using LC–MS profiling protocol

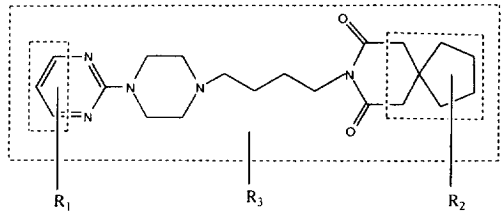

Proposed structure	No.	t^{a}_{RR}	MH^{+} [b]	Profile group[c]	R^{d}_{1}	R^{d}_{2}	R^{d}_{3}	Sample source[e]
Hydroxy buspirone glucoronide	1	0.14	594	A_s-B-P_s	+OH	+OH	+Glucoronyl	B
Hydroxy buspirone glucoronide	2	0.30	594	A_s-B-P_s	+OH	+OH	+Glucoronyl	B
Hydroxy buspirone glucoronide	3	0.35	594	A_s-B-P_s	+OH	+OH	+Glucoronyl	B
Hydroxy methoxy buspirone glucoronide	4	0.36	624	A_s-B-P_s	+OH, +OCH_3	+OH	+Glucoronyl	B
Hydroxy methoxy buspirone glucoronide	5	0.38	624	A_s-B-P_s	+OH, +OCH_3	+OH	+Glucoronyl	B
Hydroxy buspirone glucoronide	6	0.38	594	A_s-B-P_s	+OH	+OH	+Glucoronyl	B
1-Pyrimidinyl piperazine	7	0.42	165	B_s-P	U	N		S9
Buspirone glucoronide	8	0.44	578	A-B-P_s	+OH, +Glucuronyl			B
Dihydroxy buspirone	9	0.45	418	A_s-B-P	U	+2(OH)		Ur, S9
Methoxy buspirone glucuronide	10	0.46	608	A-B-P_s	+OH, +OCH_3		+Glucuronyl	B
Dihydroxy buspirone	11	0.48	418	A_s-B-P	U	+2(OH)		Ur, S9
Dihydroxy buspirone	12	0.48	418	A_s-B-P_s	+OH	+OH		Ur, S9
Despyrimidinyl peperazine buspirone	13	0.50	254	A-B_s	N	U	−Pyrimidinyl piperazine +=O, +OH	B, S9
Dihydroxy methoxy buspirone	14	0.51	448	A_s-B-P_s	+OH, +OCH3	+OH		Ur
Hydroxy buspirone	15	0.53	402	A_s-B-P	U	+OH		B, Ur, S9
Dihydroxy buspirone	16	0.55	418	A_s-B-P	U	+2(OH)		Ur
Dihydroxy buspirone	17	0.55	418	A_s-B-P	U	+2(OH)		Ur
Dihydroxy buspirone	18	0.56	418	A_s-B-P	U		+2(OH)	B
Hydroxy buspirone	19	0.59	402	A_s-B-P	U	+OH		Ur, B, S9
Hydroxy buspirone	20	0.69	402	A_s-B-P	U	+OH		Ur, B, S9
Dihydroxy buspirone	21	0.70	418	A_s-B-P_s	+OH	+OH		Ur, S9
Despyrimidinyl buspirone	22	0.74	308	A-B_s			−Pyrimidine	B
Hydroxy buspirone	23	0.74	402	A_s-B-P	U	+OH		B
Hydroxy buspirone	24	0.80	402	A_s-B-P	U	+OH		B, Ur
Hydroxy buspirone	25	0.87	402	A-B-P_s	+OH	U		Ur, S9
Buspirone	26	1.00	386	A-B-P	U	U		B, Ur, S9

[a] HPLC retention time relative to buspirone (t_{RR}=1.00) using universal HPLC conditions. Buspirone retention time was 13.5 min.
[b] Molecular mass.
[c] Refer to text for discussion of profile group categorization. A=azaspirone decane dione, B=butyl piperazine, P=pyrimidine, subscript s refers to substitution in a particular substructure, NA=not available from the data.
[d] U=unchanged substructure, N=substructure not present, BAD=butyl azaspirone decane dione.
[e] Sample source: B=rat bile in vivo, Ur=rat urine in vivo, S9=rat liver S9 preparation in vitro.

Table 2
MS–MS product ion spectra of $(M+H)^+$ ions of buspirone metabolites and interpretation.

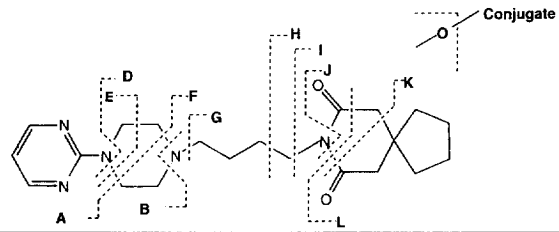

Proposed structure	Fragmentation; *m/z*																
	No.	t_{RR}	MH^+	A	B	C	D	E	F	G	H	I	J	K	L	M	Others
Hydroxy buspirone glucuronide	1	0.14	594	138												418	98
Hydroxy buspirone glucuronide	2	0.30	594	138						238						418	98
Hydroxy buspirone glucuronide	3	0.35	594	138	166				281	238						418	98
Hydroxy methoxy buspirone glucuronide	4	0.36	624	168						238					139	448	
Hydroxy methoxy buspirone glucuronide	5	0.38	624	168											139	448	
Hydroxy buspirone glucuronide	6	0.38	594	138	166				281							418	
1-Pyrimidinyl piperazine	7	0.42	165														
Buspirone glucuronide	8	0.44	578	138	164 166				265	222	180	168	152		123	402	109
Dihydroxy buspirone	9	0.45	418	122	148 150		323		297	254							
Methoxy buspirone glucuronide	10	0.46	608	168	196				265			168				432	100
Dihydroxy buspirone	11	0.48	418	122	148 150		323		297	254							
Dihydroxy buspirone	12	0.48	418	138	166				281	238							
Despyrimidinyl piperazine buspirone	13	0.50	254										151 152	95	123		236, 208, 194, 109, 86, 81
Dihydroxy methoxy buspirone	14	0.51	448	168	194 196				281	238					139		383, 121, 100
Hydroxy buspirone	15	0.53	402	122	148 150				281	238				95			98
Dihydroxy buspirone	16	0.55	418	122	148 140	177			281	238					139		400, 306, 293, 267, 98
Dihydroxy buspirone	17	0.55	418						297	238				95	139		98
Dihydroxy buspirone	18	0.56	418	122	150												98
Hydroxy buspirone	19	0.59	402	122	148 150				281	238							219, 192, 178, 98
Hydroxy buspirone	20	0.69	402	122	148 150	177			265	222	180	168	152		139		109, 108
Dihydroxy buspirone	21	0.70	418	138	164 166				281	238					139		400
Despyrimidinyl buspirone	22	0.74	308							222	180	168	152				109, 100 88, 74 59, 43
Hydroxy buspirone	23	0.74	402	122	148 150		307		281	238				95	139		168, 98
Hydroxy buspirone	24	0.80	402	122	148 150		307		281	238			168		139		98, 95
Hydroxy buspirone	25	0.87	402	138	166				265	222	180	168	152	95			109, 98
Buspirone	26	1.00	386	122	148 150		291	109	265	222	180	168	152	95			343, 109, 98

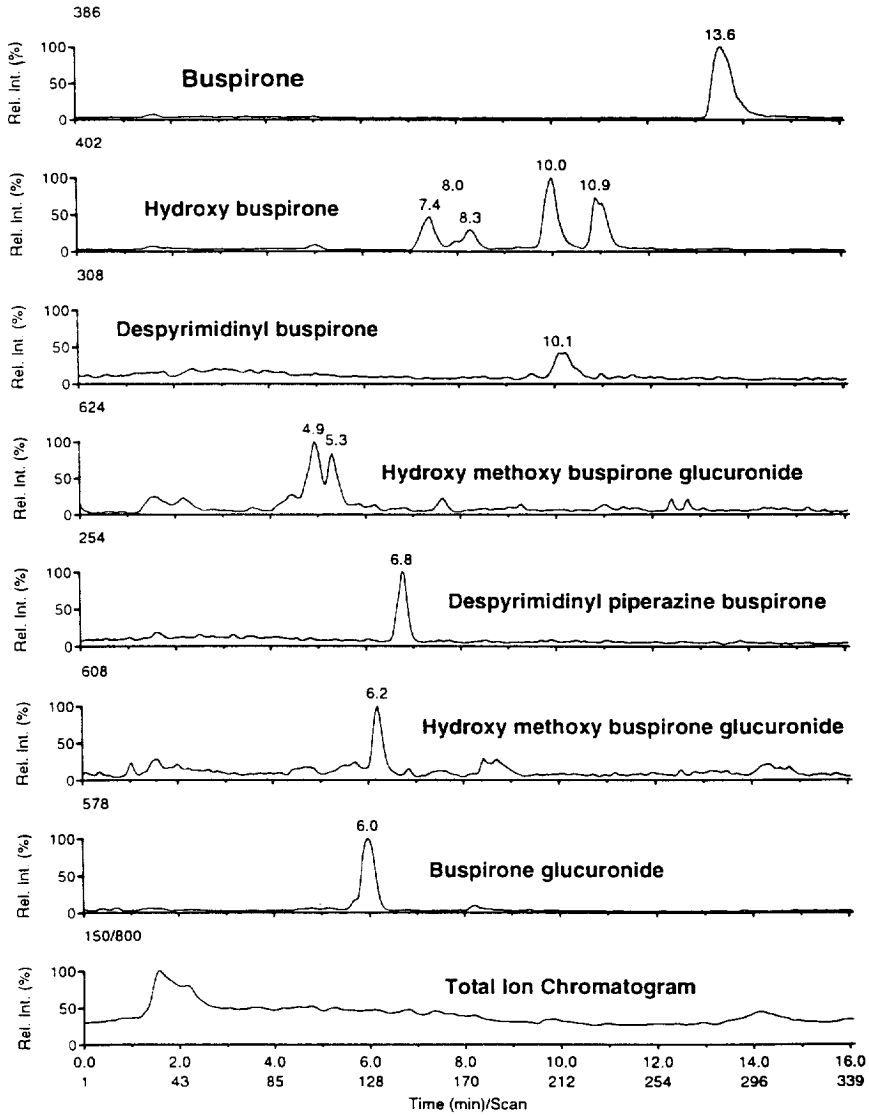

Fig. 2. Extracted ion chromatograms (mass chromatograms) of selected buspirone metabolites observed in rat bile. The ion signals plotted are shown at the left of each chromatogram. The metabolites which have been studied using MS–MS product ion spectra are noted by retention time and are listed in the tables. Minor peaks in mass chromatograms are not structurally related to buspirone or were too weak to obtain useful MS–MS product ion spectra.

P substructures with substitution occurring on the A substructure. Profile group categorization allows for the rapid recognition of the primary substructures affected by metabolic substitution. The predominant buspirone metabolite profile groups are: A_s-B-P, A-B-P_s and A_s-B-P_s, indicating A and P as metabolically active sites of attack, as well as the presence of multiple sites of substitution on each of these substructures.

An A_s-B-P profile group metabolite is illustrated in Fig. 4. The M_r increase from buspirone of 16–401 u observed in this metabolite is typically due to

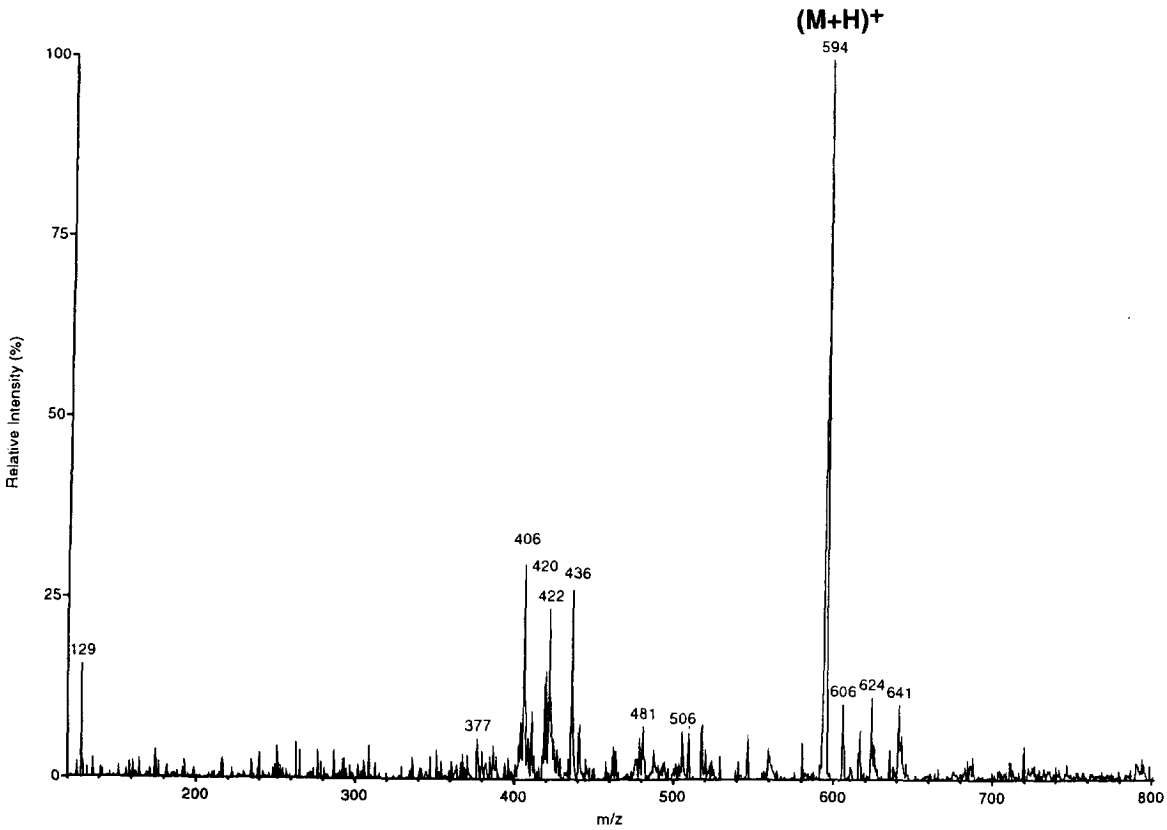

Fig. 3. Full scan ionspray mass spectrum of hydroxy buspirone glucuronide (M_r 593). No fragmentation of the labile glucuronide bond was observed at m/z 418.

hydroxylation. The presence of the m/z 122 ion indicates a metabolite structure containing an intact pyrimidine substructure. The neutral loss of 164 indicates that the metabolite contains the pyrimidinyl piperazine substructure. The m/z 180 ion is not present indicating substitution of the azaspirone decane dione substructure. Appearance of the m/z 196 ion confirms localization of the hydroxyl group on the azaspirone decane dione substructure. Shift of the azaspirone decane dione substructure at m/z 123 to m/z 139 provides complementary evidence for hydroxyl substitution on the azaspirone decane dione substructure.

Substitutions to the pyrimidine substructure are found in the A-B-P_s profile group, such as in buspirone glucuronide (Fig. 5). The increase in M_r of 192 u compared to the buspirone template is consistent with addition of glucuronic acid. The MS–MS product ion spectrum provides complementary evidence of this addition via the neutral loss of 176 (m/z 578 to m/z 402). This fragmentation is a characteristic feature of glucuronides. The difference of 16 u from m/z 122 of the template to m/z 138 localizes the position of hydroxyl substitution as the pyrimidine substructure and sequential neutral losses (m/z 578 to m/z 402 to m/z 138) indicate the molecular connectivity of the glucuronide to the pyrimidine.

The novel A-B-P_s profile group metabolite despyrimidinyl buspirone is shown in Fig. 6. The presence of the m/z 222 ion indicates the intact butyl azaspirone decane dione substructure. The 76 u M_r difference compared to the buspirone template indicates the metabolic loss of pyrimidine. Complemen-

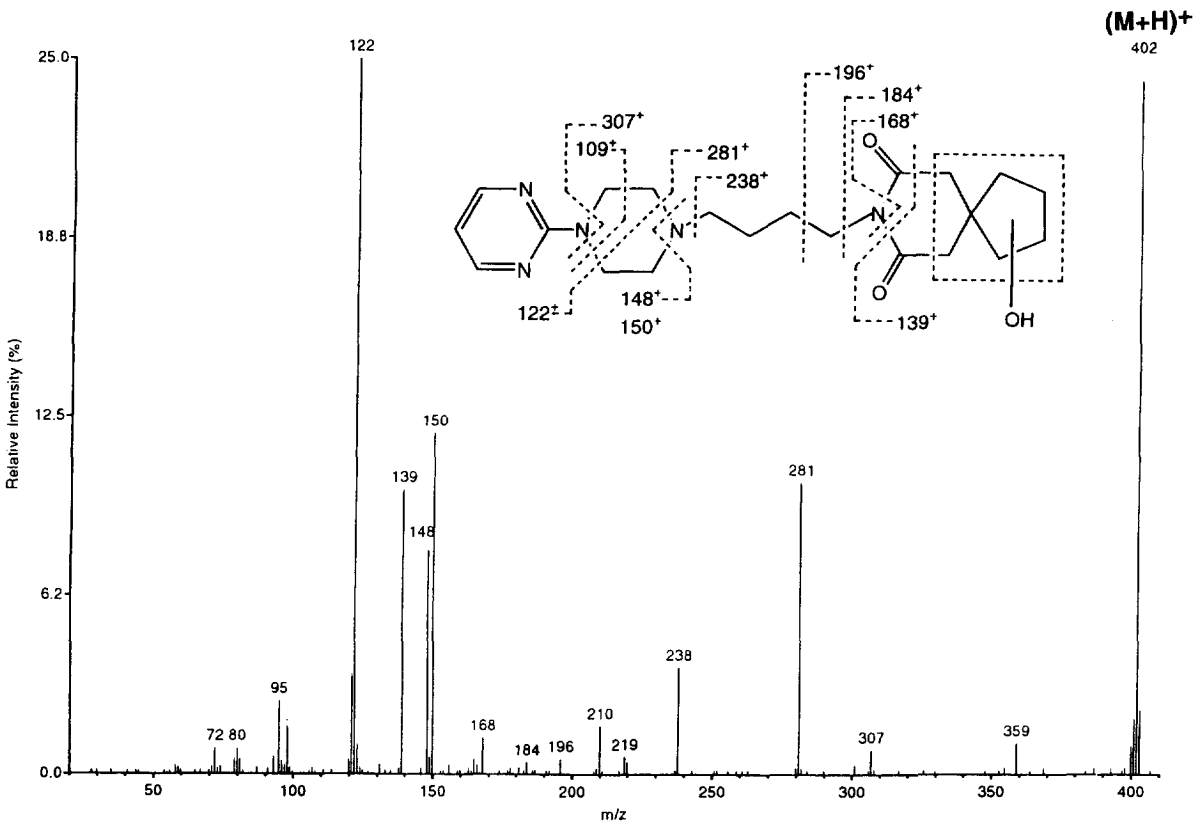

Fig. 4. Structure and ionspray MS–MS product ion spectrum of m/z 402 $(M+H)^+$ of hydroxy buspirone, substituted on the azaspirone decane dione substructure.

tary evidence for absence of the pyrimidine substructure is the absence of the m/z 122 ion. The sequential ions at m/z 43, 57, 74, 88 and 101 provide complementary molecular connectivity evidence for the piperazine substructure.

Another novel metabolite structure identified in this study is despyrimidinyl piperazine buspirone (azaspirone decane dione N-butyric acid). The m/z 152 and 123 ions indicate that this structure contains the azaspirone decane dione substructure. The sequential ions at m/z 236, 208, 194, 180, 152, 123, 109, 95, 81 are indicative of molecular connectivity along the butyric acid sidechain and throughout the azaspirone decane dione substructure. This metabolite provides evidence for the metabolic fate of the portion of the buspirone structure cleaved off to form 1-pyrimidinyl piperazine, which has been well characterized [22–25].

4. Conclusions

A detailed database of buspirone metabolite structures has been obtained using a rapid LC–MS strategy. LC–MS analysis provides a comprehensive metabolite structure profile, as well as the t_{RR}, M_r and UV characteristics of each metabolite. LC–MS–MS product ion data of each metabolite component provides detailed substructural information characteristic of its structure. The metabolite profile reveals the primary modes of buspirone metabolic decomposition (i.e., hydroxylation, glucuronidation, N-dealkylation), as well as the primary substructures affected by metabolic reactions (i.e., azaspirone decane dione and pyrimidine). This database is useful for the rapid dereplication and elucidation of metabolites observed in future samples, such as from clinical studies. Many of the elucidated structures are

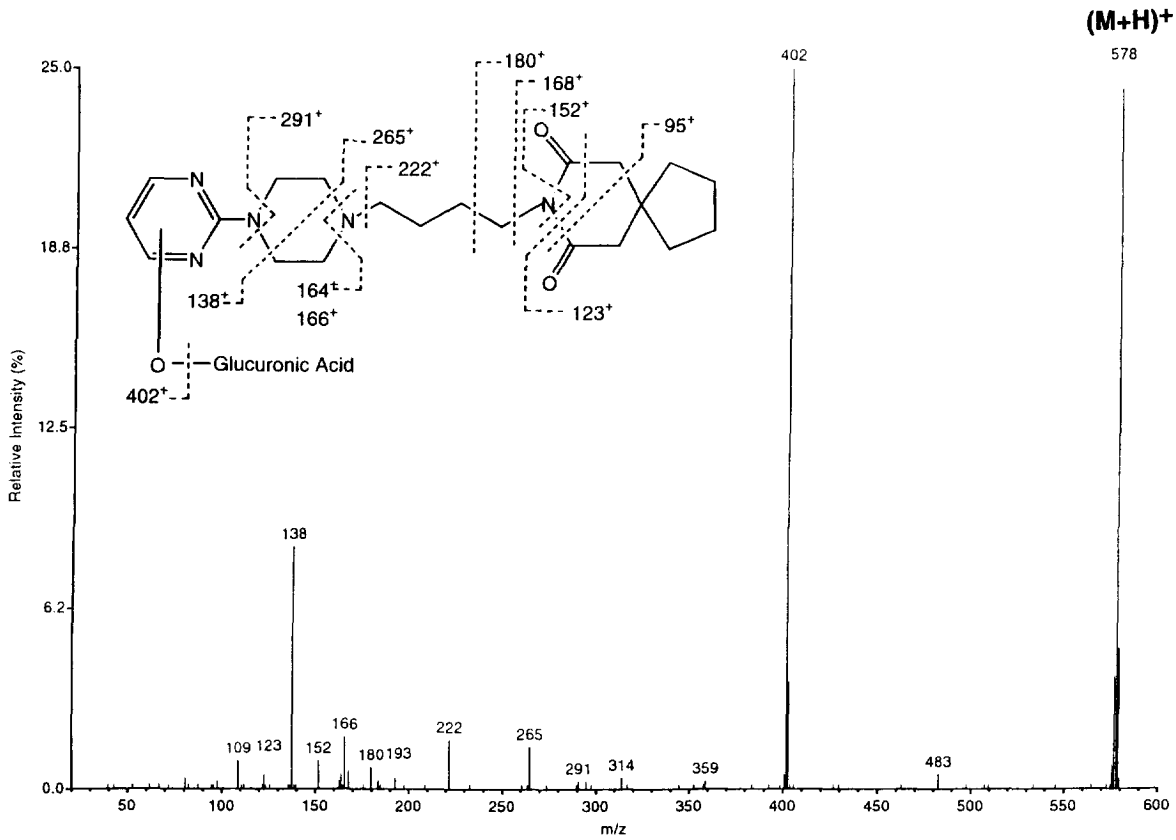

Fig. 5. Structure and ionspray MS–MS product ion spectrum of m/z 578 $(M+H)^+$ of buspirone glucuronide, substituted on the pyrimidine substructure.

definitive, such as in the case of despyrimidinyl buspirone. For others, all of the possible isomers are observed (e.g., hydroxy-pyrimidinyl buspirone). In other cases the position of substitution on a substructure is not specifically indicated, however, such detail is often unnecessary for timely support of discovery research in an accelerated research environment. It is often advantageous to use LC–MS profile information to proceed directly to following stages of chemical synthesis.

This LC–MS protocol consistency provides broad-based applicability for a wide range of drug candidate classes and metabolite polarities. The observation of new buspirone metabolites, as well as those previously known, demonstrates the breadth of the procedure. The despyrimidinyl metabolites would not have been observed in studies relying on radioactive labelling of the pyrimidine substructure. Similarly, the intact glucuronide conjugates would not have been observed in studies relying on enzymatic deconjugation or more energetic methods. The low energy ionspray interface allows for the observation of labile metabolites and interfacing with a broad gradient HPLC method, provides for an accurate and complete survey of the diverse metabolite profile. Neither synthesized standards, radiolabeled drug, nor complex sample preparation steps were necessary for detection, characterization or identification of metabolites using this procedure.

The use of standard conditions, locked-in early in the development cycle, permits consistent analysis of samples and applicability of structure database information throughout the lifetime of a product, extending to support of activities in research, development, production and clinical therapy. The approach insures high speed and increased prod-

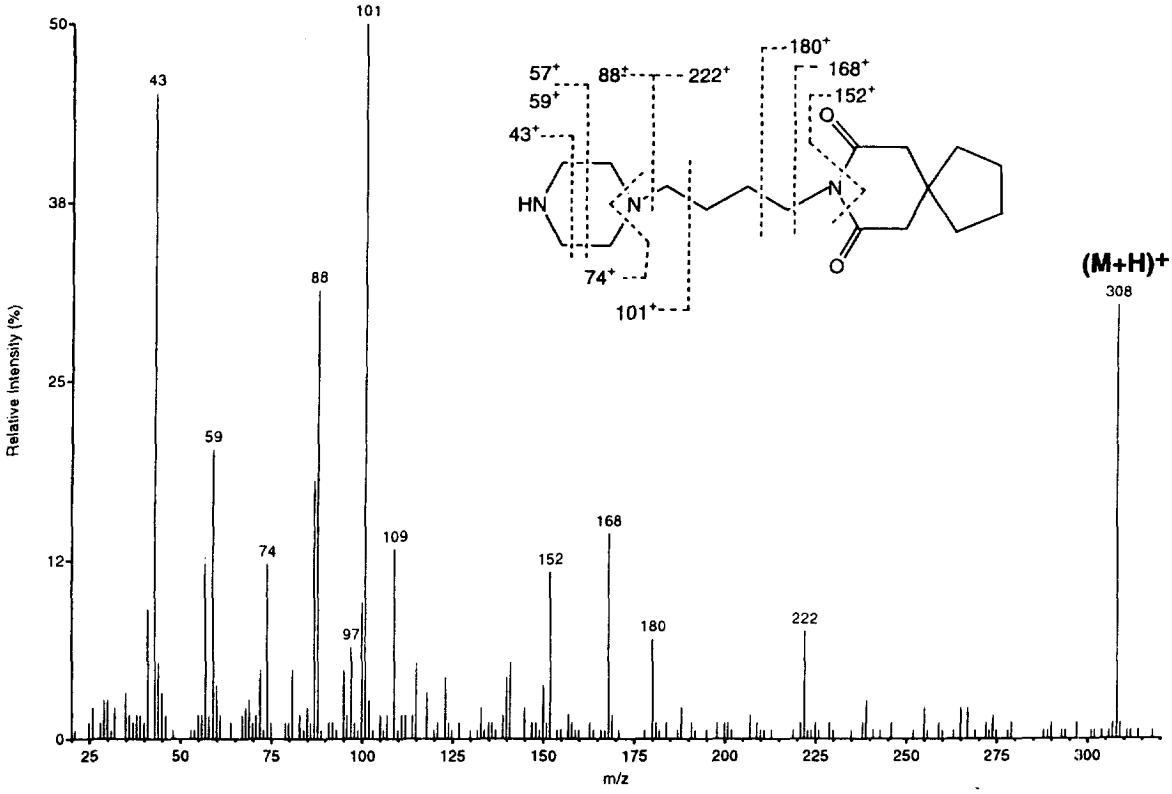

Fig. 6. Structure and ionspray MS–MS product ion spectrum of m/z 308 $(M+H)^+$ of despyrimidinyl buspirone.

uctivity. The studies discussed here incorporated three sample matrices and required approximately one day to complete (10 min for sample preparation, automated overnight LC–MS analysis, 1.5 h per sample for LC–MS–MS substructural analysis and 1.5 h per sample for data interpretation). As a result of increased speed and throughput, this strategy provides early access to detailed information for candidate selection. This same procedure is also useful for the generation of structure databases for accelerated research programs dealing with natural products [1–3], combinatorial libraries, drug impurities [2] and drug stability [4,5] and, thus providing a universal strategy applicable to high-throughput multidisciplinary support.

Acknowledgments

The authors wish to gratefully acknowledge the contributions of collaborators in this project. Ira E. Rosenberg and Jerry R. Allison supported these studies with valuable resources. Samples were kindly provided by Carol Cole and Robert Mayol. Steven E. Klohr provided helpful assistance in reviewing the manuscript.

References

[1] M.S. Lee, D.J. Hook, E.H. Kerns, K.J. Volk, I.E. Rosenberg, Biol. Mass Spectrom. 22 (1993) 84.
[2] E.H. Kerns, K.J. Volk, S.E. Hill, M.S. Lee, J. Nat. Prod. 57 (1994) 1391.
[3] E.H. Kerns, K.J. Volk, S.E. Hill, M.S. Lee, J. Rapid Commun. Mass Spectrom. 9 (1995) 1539.
[4] K.J. Volk, S.E. Klohr, R.A. Rourick, E.H. Kerns, M.S. Lee, J. Pharm. Biomed. Anal. 14 (1996) 1663.
[5] R.A. Rourick, K.J. Volk, S.E. Klohr, T. Spears, E.H. Kerns, M.S. Lee, J. Pharm. Biomed. Anal. 14 (1996) 1743.
[6] P. Rudewicz, K.M. Straub, Anal. Chem. 58 (1986) 2928.
[7] T.J.A. Blake, I.G. Beattie, Biomed. Environ. Mass Spectrom. 18 (1989) 637.

[8] G.C. DiDonato, S.J. Gaskell, in T. Matsuo, R.M. Caprioli, M.L. Gross, Y. Seyama (Editors), Biological Mass Spectrometry Present and Future, Wiley, New York, NY, 1994, p. 541.
[9] T.A. Baillie, Int. J. Mass Spectrom. Ion Processes 118/119 (1992) 289.
[10] D.W. Everett, T.J. Chando, G.C. DiDonato, S.M. Singhri, H.Y. Pan, S.H. Weinstein, Drug Metab. Dispos. 19 (1991) 740.
[11] W.M. Muck, J.D. Henion, Biomed. Environ. Mass Spectrom. 19 (1990) 37.
[12] L. Weidolf, T.R. Covey, Rapid Commun. Mass Spectrom. 6 (1992) 192.
[13] A.E. Mutlib, J.T. Strupczewski, S.M. Chesson, Drug Metab. Dispos. 23 (1995) 951.
[14] R.J. Perchalski, R.A. Yost, B.J. Wilder, Anal. Chem. 54 (1982) 1466.
[15] R.J. Perchalski, M.S. Lee, R.A. Yost, J. Clin. Pharmacol. 26 (1986) 435.
[16] M.S. Lee, R.A. Yost, R.J. Perchalski, Annu. Rep. in Med. Chem. 21 (1986) 313.
[17] M.S. Lee, R.A. Yost, Biomed. Environ. Mass Spectrom. 15 (1988) 193.
[18] A. Bruins, T.R. Covey, J.D. Henion, Anal. Chem. 59 (1987) 2642.
[19] D.L. Temple Jr., J.P. Yevich, J.S. New, J. Clin Psychiatry 43 (1982) 4.
[20] L.A. Riblet, D.P. Taylor, M.S. Eison, H.C. Stanton, J. Clin Psychiatry 43 (1982) 11.
[21] R.E. Gammans, E.H. Kerns, W.W. Bullen, J. Chromatogr. 345 (1985) 285.
[22] R.E. Gammans, R.E. Johnston, in G. Tunnicliff, A.S. Eison, D.P. Taylor (Editors), Buspirone: Mechanisms and Clinical Aspects, Academic Press, San Diego, CA, 1991.
[23] H. Jajoo, R. Mayol, J. LaBudde, I. Blair, Drug Metab. Dispos. 17 (1989) 625.
[24] H. Jajoo, R. Mayol, J. LaBudde, I. Blair, Drug Metab. Dispos. 17 (1989) 634.
[25] H.K. Jajoo, I.A. Blair, L.J. Klunk, R.F. Mayol, Xenobiotica 8 (1990) 779.